Absolute cross sections for elastic electron scattering from 3-hydroxytetrahydrofuran

2008 New J. Phys. 10 103005

(http://iopscience.iop.org/1367-2630/10/10/103005)

New Journal of Physics
The open-access journal for physics

Absolute cross sections for elastic electron scattering from 3-hydroxytetrahydrofuran

A R Milosavljević[1,4], F Blanco[2], J B Maljković[1], D Šević[1], G García[3] and B P Marinković[1]

[1] Laboratory for Atomic Collision Processes, Institute of Physics, Pregrevica 118, 11080 Belgrade, Serbia
[2] Departamento de Física Atómica Molecular y Nuclear, Facultad de Ciencias Físicas, Universidad Complutense, Avda. Complutense s/n, E-28040 Madrid, Spain
[3] Instituto de Matemáticas y Física Fundamental, Consejo Superior de Investigaciones Científicas, Serrano 121, 28006 Madrid, Spain
E-mail: vraz@phy.bg.ac.yu

New Journal of Physics **10** (2008) 103005 (19pp)
Received 2 August 2008
Published 2 October 2008
Online at http://www.njp.org/
doi:10.1088/1367-2630/10/10/103005

Abstract. The results of measurements and calculations of absolute cross sections for elastic electron scattering from the 3-hydroxytetrahydrofuran (3hTHF) ($C_4H_8O_2$) molecule are reported. The measurements were performed using a crossed beam experimental setup, for an incident electron energy range of 40–300 eV and an overall scattering angle range of 10°–110°. Relative differential cross sections (DCSs) were measured both as a function of the angle and the incident energy and the absolute DCSs were determined using the relative flow technique. The calculations of molecular cross sections are based on a corrected form of the independent-atom method, known as the screen corrected additivity rule (SCAR) procedure and using an improved quasifree absorption model. Additional calculations are also done to investigate the influence of rotational excitations and low-angular behavior of SCAR DCSs. The calculated dataset includes differential, integral and total cross sections in the energy range from 5 eV to 10 000 eV. The present results are discussed regarding the most recent low-energy elastic DCSs for 3hTHF (Vizcaino *et al* 2008 *New J. Phys.* **10** 053002), as well as the recent DCSs for molecules of similar structure (tetrahydrofuran and tetrahydrofurfuryl alcohol).

[4] Author to whom any correspondence should be addressed.

Contents

1. Introduction

There has been increasing interest in recent years in investigating electron interactions with the 3-hydroxytetrahydrofuran (3hTHF) molecule ($C_4H_8O_2$, 3-furanol, tetrahydro-). The motivation predominantly comes from radiation damage research, since 3hTHF may be regarded as a structural analogue to the deoxyribose sugar, which forms the backbone of DNA (see figure 1). It has been shown already that low-energy secondary electrons, formed on the track of the primary ionizing particle, can efficiently induce further damage of large biomolecules [1, 2]. Actually, due to the large number of the formed secondary electrons, they carry most of the energy deposited in the tissue, so in order to deeply understand the final biological damage on a macroscopic level, it is of particular importance to investigate electron driven processes on a microscopic level. With this motivation, a number of studies, both experimental and theoretical, on electron interaction with the building blocks of DNA or their structural analogues have been reported in recent years. Here, the studying of the model molecules offers several advantages, such as the possibility to investigate selectively the importance of different molecular subunits, a clear physical picture and more favorable experimental conditions.

Although a large number of papers have been published only in a few recent years devoted to the electron interaction with (deoxy)ribose analogue compounds, they are mostly focused on the simplest tetrahydrofuran (THF) molecule, while existing results for 3hTHF are still rather scarce. The latter include theoretical calculations of differential and integral cross sections (ICSs) for elastic collisions using the independent atom method (IAM) [3], investigation of the 5–40 eV electron stimulated desorption yields of H^- produced by dissociative electron attachment (DEA) to 3hTHF physisorbed on a polycrystalline Pt substrate [4, 5], the investigation of DEA to gaseous 3hTHF [6] and, very recently, total cross section (TCS) measurements for positron scattering from 3hTHF [7] and a study on electron impact ionization of 3hTHF [8]. According to our knowledge, the first (and only) measured absolute differential cross sections (DCSs) for elastic electron scattering from 3hTHF were published very recently by Vizcaino *et al* [9], for incident energies up to 20 eV.

The present results bring an extension to the existing data in several directions. Firstly, they extend the recently published [9] experimental low-energy (6.5–20 eV) absolute DCSs for elastic electron scattering from 3hTHF up to 300 eV, as well as theoretical absolute

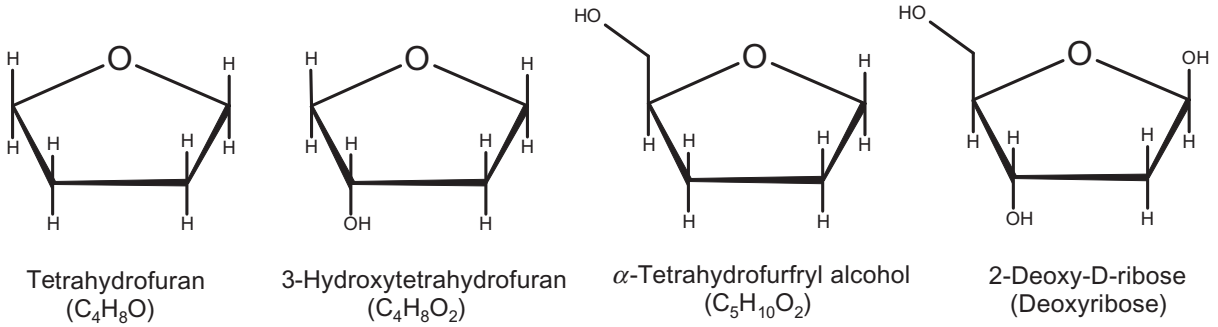

Figure 1. Schematic drawing of THF, 3hTHF, α-THFA and 2-deoxy-D-ribose (deoxyribose) molecules.

cross sections up to 10 000 eV. Furthermore, they also complete up our previous work on the molecules of similar structure: THF [10] and tetrahydrofurfuryl alcohol (THFA) [11] (see figure 1). Therefore, it is possible to study the elastic electron scattering processes for different structurally similar molecules, starting from the simplest THF (an ether, representing a saturated furanose ring), through the more complex 3hTHF (an alcohol, where one H atom in THF is substituted by an OH group) and THFA (an alcohol, where one H atom in THF is substituted by a CH_2OH group), so further to extrapolate some conclusions to the more complex biologically relevant compounds, e.g. deoxyribose (a sugar, containing both OH and CH_2OH groups attached to the furan ring). Also, the presented work tests the possibility of different theoretical approaches to calculate DCSs for elastic scattering from the abovementioned molecules.

In this work, similarly as previously for THF and THFA, an advantage of the screen corrected additivity rule (SCAR) procedure over the classical IAM and a very good agreement of experimental and theoretical absolute DCSs have been shown in the medium energy range (here 40–300 eV). Furthermore, two additional sets of calculated DCSs are presented and discussed in this paper. One is obtained according to a normalized SCAR procedure in order to reduce the interference terms as much as necessary to ensure that integrated elastic values also satisfy the (corrected) additivity rule (which is a known limitation of the IAM). The other accounts for the rotational excitations which could be important for a molecule with a high permanent dipole moment. The three sets of calculated DCSs were compared with the present experiment, regarding both the absolute values and the DCS shape.

According to our knowledge, this paper reports the first experimentally obtained absolute DCSs for elastic scattering of electrons from 3hTHF in the energy range from 40 eV to 300 eV. The final DCS dataset has been obtained by merging the three independent sets of experimental results (obtained by measuring independently relative DCSs as a function of either the scattering angle or the incident energy and absolute DCSs using the relative flow technique) and is additionally accompanied by SCAR calculations, which show a very good agreement with the experiment.

2. Experiment

The measurements were performed on a crossed electron–molecular target beam apparatus, which has been described in detail previously [12]. Therefore, only a brief description of

the experimental system and a procedure for relative DCS measurements will be given here. Furthermore, the apparatus has been recently upgraded to apply the relative flow technique for measurements of absolute DCSs, as well, so this part will be described in more detail.

The experimental setup includes an electron gun producing a well collimated, nonmonochromated incident electron beam, which is crossed perpendicularly by a molecular target beam produced by a stainless steel needle. The gun can be rotated around the needle in the angular range from about -40° to 120°. The scattered electrons are retarded and focused by a four-element cylindrical electrostatic lens into a double cylindrical mirror analyzer, followed by a three-element focusing lens and a single channel electron multiplier working in a single electron counting mode. The base pressure of about 3×10^{-7} mbar was obtained by a turbo-molecular pump. The uncertainty of the incident energy scale was determined to be less than ± 0.4 eV, by observing a threshold for He^+ ions yield. The best energy resolution of about 0.5 eV is limited by the thermal spread of primary electrons. The angular resolution was better than $\pm 2^\circ$.

The anhydrous 3hTHF was purchased from Merck KGaA with a declared purity better than 98% and was used after several degassing cycles under vacuum, which were performed before each set of measurements. It was introduced into the scattering region from a glass container via a gas line system, which was recently upgraded (new line design with diverting valves, absolute pressure gauge, temperature-controlled heating etc) to allow efficient and stable relative flow measurements, as well as more efficient measurements of relative DCSs. Here, it is important to emphasize particular experimental difficulties connected with the 3hTHF molecule. These are partly due to general problems with polar 'sticky' molecules, as already reported recently in more detail for THF by Allan [13] (the 1.67 Debye [9] dipole moment of 3hTHF is very close to that of THF). If a certain fraction of the sample (as a function of pressure) is adsorbed on the inner walls of the gas line–pressure gauge system, it could influence the flow of the sample gas, thus resulting in an unstable target beam and, especially, inducing problems in relative flow measurements (see below). Furthermore, in the case of 3hTHF, additional difficulties arise due to a very low vapor pressure of this molecule at room temperature (less than 1.3 mbar), which is, e.g. more than two orders of magnitude lower than for THF. This was also pointed out in the most recent paper by Vizcaino *et al* [9], who heated the whole gas-handling system and the needle to a temperature of 90 °C in order to produce a stable driving pressure for the beam and a high-enough signal. However, Vizcaino *et al* [9] also noted that this hot sample beam would contain a significant fraction of rotationally and vibrationally excited molecules, which in principle can influence the measured elastic DCS values. In the present experiment the whole gas-handling system (sample container, pipes, valves and needle) was also heated, which is a necessary requirement to provide stable experimental conditions. We have introduced a small temperature gradient in order to prevent, as much as possible, the condensation of the sample vapor on the inner walls of the gas system. Therefore, the sample container was kept at a temperature of about 60 °C, the following pipes and valves at about 60–65 °C and finally the needle at about 70 °C. The temperature gradient was still kept relatively small, so as not to disturb relative flow measurements, as discussed before [14]. It should be noted, finally, that because of the energy resolution of about 0.5 eV in the incident electron beam, the 'elastic' DCSs measured in the present experiment also inevitably include the rotational and vibrational excitations.

The relative DCSs were measured both as a function of the scattering angle and the incident electron energy, according to the procedure already described before [12]. The adjusted

driving pressures behind the nozzle were typically 0.13–0.47 mbar (measured by a temperature controlled type MKS Baratron gauge), which correspond to the working pressures in the vacuum chamber of about $3.5–8.5 \times 10^{-6}$ mbar. For each experimental point, the measured signal intensity was normalized to the driving pressure which was simultaneously acquired (it should be noted, however, that these corrections were usually practically negligible, since the pressure was very stable during one relative DCS measurement). The background contributions, which were measured after redirecting the gas flow through the side leak, were subtracted for each measured electron yield. The background contributions were generally more important at low incident energies and scattering angles, as well as close to DCS minima, but were typically below 10% and practically negligible at higher incident energies (>100 eV). In the case of measurements performed as a function of the electron energy, special care has been taken to preserve, as much as possible, constant electron beam geometry and transmission function (see [12]). For both types of relative measurements (as a function of angle or energy), the experimental procedure was checked and possible small corrections have been made according to benchmark DCSs for Kr [15]–[19], which were measured under the same experimental conditions, for all the applied incident energies or fixed scattering angles.

The measured relative DCSs are normalized to the absolute scale according to the relative flow method [20, 21]. This method is based on measurements of intensities for elastic scattering by a reference gas and the gas under study, at a given incident electron energy (E) and scattering angle (θ), under experimental conditions where these intensity ratios can be accurately established, so allowing determination of the absolute DCS of the gas under study according to the known elastic DCS for the reference gas. It has been shown [21] that if the flows from the needle are identical for both gases (resulting in the same beam profile in the collision region), the absolute cross section for the gas under study (here 3hTHF) can be obtained according to the following formula:

$$\mathrm{DCS}_{\mathrm{3hTHF}}(E,\theta) = \mathrm{DCS}_{\mathrm{R}}(E,\theta)\frac{N_{\mathrm{3hTHF}}F_{\mathrm{R}}}{N_{\mathrm{R}}F_{\mathrm{3hTHF}}}\sqrt{\frac{M_{\mathrm{R}}}{M_{\mathrm{3hTHF}}}}. \quad (1)$$

Here, $\mathrm{DCS}_{\mathrm{3hTHF}}(E,\theta)$ and $\mathrm{DCS}_{\mathrm{R}}(E,\theta)$ represent absolute DCSs for elastic electron scattering from the 3hTHF molecule and the reference atom; N_{3hTHF} and N_{R} are measured signal intensities; F_{3hTHF} and F_{R} are measured mass flow rates; and M_{3hTHF} and M_{R} are molecular (atomic) weights, respectively. According to a commonly accepted procedure suggested by Nickel *et al* [21], in order to obtain the same beam profile the driving pressures behind the nozzle of the used gasses should be adjusted such that the mean free paths are equal (according to their gas-kinetic diameters) and longer than the nozzle diameter.

In the present experiment, Kr is used as a reference gas. The 3hTHF molecule and Kr possess similar atomic weights and similar gas-kinetic diameters (also resulting in similar mass flow rates), which makes it easier to obtain similar experimental conditions and to perform accurate measurements, thus reducing the overall error. For example, using He as a reference gas would require a much higher ratio of driving pressures (He to 3hTHF) but due to a significantly higher mass flow rate of He, practical difficulties arise from having a very low working pressure of 3hTHF (and, thus, low signals) and a short time to measure the flow rate for He gas (see details below). Finally, using Kr is also convenient for testing the relative DCS measurements as a function of energy (discussed above), since experimental DCSs exist for elastic electron–Kr scattering reported in small energy steps up to about 250 eV [15, 16].

For the present experiment, the ratio of driving pressures behind the nozzle is determined to be $p_{\mathrm{Kr}} : p_{3\mathrm{hTHF}} = 1.36 : 1$. Here, the value for the gas-kinetic diameter of 3hTHF has been taken according to the reference for the linear isomer of this molecule—ethyl acetate [22]. Note that even if the real diameter was slightly different from the applied one, the resulting error would be negligible in comparison with that given by both the precision and the stability of the pressure for a molecule like 3hTHF. The influence of a variation of the applied driving pressure ratio to the measured absolute cross section depends on the characteristics of the experimental setup but should not be dramatic. In the previous works for the THF molecule, Dampc *et al* [14] reported that variations of this pressure ratio did not change absolute DCSs within measured uncertainties, while more recently Allan [13] has performed a more detailed measurement which showed that even a deviation of the applied ratio of a factor of 2 from the optimal value changes the measured absolute DCS by less than ±15%. In the present study, we have taken into account only those relative flow measurements where the ratios of the driving pressures were within ±20% of the derived value of 1.36. The driving pressure for 3hTHF applied for the relative flow measurements was usually about 0.2 mbar. The mass flow rates of the gases (F_{Kr} and $F_{3\mathrm{hTHF}}$) have been measured by closing the outlet to the gas chamber and recording the increase of the absolute pressure in the gas line behind the needle as a function of time (using an automated acquisition controlled by a PC LabView program). The obtained experimental curves were then fitted to a linear function by a least squares method to obtain the flow rate. It should be noted that both for Kr and 3hTHF the increase of the pressure versus time showed strong linearity, with a correlation coefficient always close to 1 within 1%. For each experimental point, both the signal and the background intensities were repeatedly measured and the final intensities (N_{Kr} and $N_{3\mathrm{hTHF}}$) were obtained by subtracting the mean background value from the mean signal value. The background contributions were typically 2% to 10% and only at lower incident energies and close to DCS minima increased up to about 15%. Note that for relative flow measurements the background contains both gases (Kr and 3hTHF), which were redirected through either the needle or the side lick.

Finally, it is important to point out that the final set of absolute DCSs should be consistent with respect to all three sets of independent experimental results: relative angle-DCSs measured at fixed incident electron energies, relative energy-DCSs measured at fixed scattering angles and, finally, absolute DCSs measured at both fixed incident energy and scattering angle. Crossing all these results allows one to find possible errors in the applied experimental procedure, as well as inconsistencies in the reference cross section data set. However, as the relative flow method imposes, the uncertainty of the absolute position of the final cross section surface still depends on the absolute error of the used reference DCSs.

2.1. Error discussion

The errors for the relative DCSs measured as a function of the scattering angle include statistical errors (0.1–3%), according to Poisson's distribution and short-term stability errors (1–3%), according to the discrepancy of repeated measurements at the same incident energy and scattering angle. Therefore, the overall error of the relative angle-DCSs is estimated to be up to 5%. This error is enlarged only for the scattering angles below 20° to up to approximately 10%, due to the possible uncertainty of a change of the effective scattering volume.

The errors for the relative DCSs measured as a function of the incident electron energy also include statistical errors (0.1–3%) and short-term stability errors (1–5%). Furthermore, since

the final relative DCSs were obtained after applying corrections as a function of the incident energy, according to benchmark measurements for Kr, this introduces an error of up to 6% due to an uncertainty of the relative benchmark DCSs. Therefore, the overall error of the relative energy-DCSs is estimated to be up to 7%.

The error of an absolute DCS obtained by the relative flow technique at a certain fixed incident energy and scattering angle depends on the absolute error of the reference DCS used for calibration and the errors of measurements of the signal intensity and the flow rate (see formula (1)). The latter errors (for the flow rate and the signal intensity) introduce small uncertainty, so the overall error is dominantly defined by the error of the reference absolute DCS. The final signal intensities were obtained after extracting the background contribution, so the final errors for the signal intensities include both statistical errors (for the signal and the background). However, due to high counting rates and low background, these errors were less than 5%. The errors for the measured flow rates were practically negligible due to stable experimental conditions and a strong linear increase of the pressure in time. However, the reported errors for the reference absolute DCSs for Kr which have been used for calibration are 20%, which also define a minimal uncertainty of the present results. The absolute errors of the present absolute values are further enlarged by the calibration error, depending on the possible variations on the absolute scale either of angle-differential or energy-differential relative cross sections when fitted to one or several absolute points. Therefore, we estimate the final overall error of the present absolute DCSs to be up to 25%.

3. Calculations

Present calculations of molecular cross sections are based on a corrected form of the IAM, known as the SCAR procedure, with an improved quasifree absorption model potential, which includes relativistic and many-body effects, as well as inelastic processes. The SCAR procedure has been extensively described in the previous work [23]. In the standard IAM approximation the electron–molecule collision is reduced to the problem of collision with individual atoms by assuming that each atom of the molecule scatters independently and that redistribution of atomic electrons due to the molecular binding is unimportant. At low energies, where atomic cross sections are not small compared to (squared) interatomic distances in the molecule, the IAM approximation fails because the atoms can no longer be considered as independent scatterers and multiple scattering within the molecule is not negligible. These large low-energy atomic cross sections would overlap inside the molecule if geometrically visualized. As a result the atoms screen each other from the incident electrons, and the molecular cross section is no longer the sum of atomic ones. The role of SCAR correction is just reducing the values obtained from the standard additivity rule for those geometrical overlappings.

The SCAR procedure has improved the IAM method to account for the overlapping of the atomic cross sections of the target molecule and has shown very good agreement with the experiment in the present energy and angular ranges. However, it still suffers from a general problem of the IAM procedures when applied to differential calculations, which is an overestimation of the resulting interference contributions at small angles. This also causes the integrated elastic cross section not to satisfy the additivity rule. Therefore, in the present paper we also introduce an additional set of theoretical DCSs where interference terms were normalized (reduced) as much as necessary to ensure that integrated elastic values also satisfy the (corrected) additivity rule (the SCARN procedure in the following). The main effect of that

correction is an appreciable reduction of the differential elastic values at small angles, while generally only small deviations from SCAR calculations are seen at higher angles.

Both SCAR and SCARN methods ignore the rotational and vibrational excitations and consider only those inelastic processes arising from electronic excitation. Although this restriction is not significant in general for the relatively high energies (as used in the present work), in the case of molecules with a relatively high permanent dipole moment, rotational excitation becomes more important (see the recently published work on the water molecule [24] and references therein). Therefore, in the present work, we also introduce a further set of calculated DCSs where a previously applied procedure [24] has been used to account for this effect (SCARND procedure in the following). The method consists of the calculation of the rotational excitation cross section for a free electric dipole by assuming that the energy transferred is low enough, in comparison with the incident energy, to validate the first Born approximation. In these conditions, we have calculated an average rotational excitation cross section $J \rightarrow J'$ for 3hTHF at 300 K by weighting the population of the J rotational quantum number at that temperature and estimating the average excitation energy from the corresponding rotational constants. The most important effect of this correction is the increase of the absolute value of the cross section, which is significant at low incident energies and small scattering angles.

4. Results and discussion

4.1. Relative angle-DCSs

Before discussing the absolute cross section values, it is interesting to investigate the relative behavior of the DCSs regarding both different molecules of similar structure which have been used to model deoxyribose (see section 1) and different theoretical approaches which have been applied in this energy range to calculate the cross sections (see section 3). Firstly, we would like to gain some conclusions about a dependence of the shape of the DCS on a variation of the molecular structure upon changing the group of atoms attached to the furanose ring. Secondly, we are interested in the possibility of different variations of the IAM procedure to reproduce the DCS shape in fine detail.

In figure 2, both experimental and theoretical relative DCSs are presented at several incident electron energies from 50 eV to 300 eV. The DCSs are normalized to each other to obtain the best overall fitting of the curves. The experimental DCSs include the present results for 3hTHF molecule (full circles), as well as the previously published data for THF (open squares [10]) and THFA (open triangles [11]). It is obvious that DCSs for all three molecules show practically the same relative behavior at all electron energies presented in figure 2 (this statement stands also for the other energies where DCSs are not presented). Only slight differences which can be seen close to the DCS minima are induced by experimental imperfections, according to our opinion, and are most probably due to somewhat higher influence of the background in the previous measurements. The DCSs are characterized by a small shoulder around 35°–55° and a broad minimum in the range 80°–100° which is most pronounced at an energy of about 100 eV and disappears at higher energies. The same shapes of the experimental DCSs for all three molecules lead to the conclusion that a substitution of the H atom in THF by either OH or CH_2OH groups does not influence the relative behavior of the DCSs. This also suggests that a cross section for the simplest analogue molecule (e.g. THF)

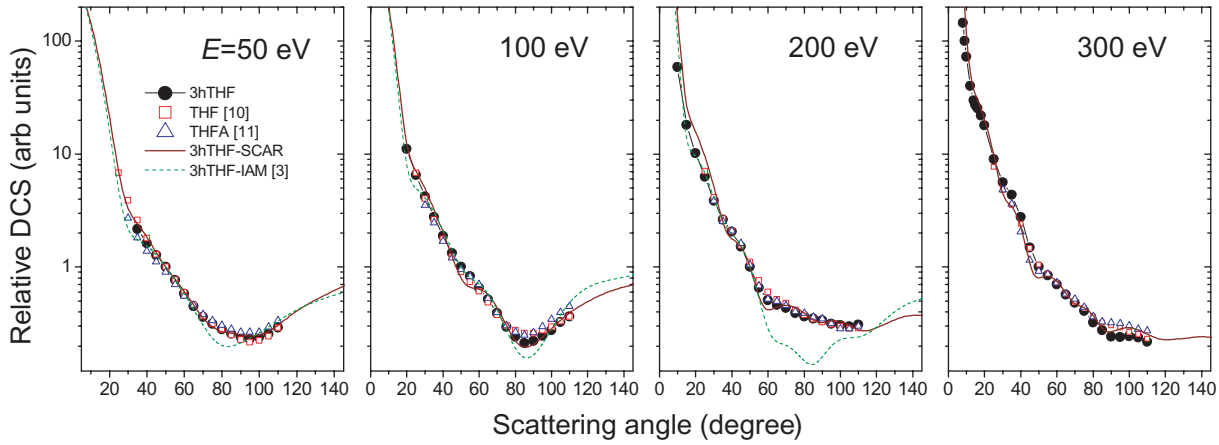

Figure 2. Comparison of relative experimental DCSs for elastic electron scattering from 3hTHF (full circles—present results), THF (open squares—Milosavljević *et al* [10]) and THFA (open triangles—Milosavljević *et al* [11]) molecules, as well as relative theoretical cross sections for 3hTHF (full line—present SCAR procedure; dashed line—Možejko and Sanche [3]). The relative cross sections are normalized to each other to obtain the best overall fitting of the curves. The errors of the experimental relative cross sections are within the size of the symbols.

might be used to estimate the DCS behavior of an even more complex biologically relevant compound (e.g. deoxyribose).

The theoretical DCSs are presented in figure 2 only for the 3hTHF molecule and have been obtained using either the IAM (dashed curves [3]) or the present SCAR (full curves) procedure. Generally, both these methods, based on the independent atom model, reproduce very well the measured relative behavior of the DCSs for elastic electron–3hTHF scattering, in the energy and angular ranges used. Still, the present SCAR calculations are clearly more favorable, while the previously applied uncorrected IAM method [3] shows deviations from the experimental data close to the DCS minima (which is especially pronounced at 200 eV) and at high angles. The same general conclusion about SCAR and IAM procedures has been also confirmed previously for THF and THFA [10, 11]. Finally, note that the present calculations reproduce even some fine details of the DCSs, such as a small maximum at about 100° for 300 eV, which is also revealed by the present measurements where special care has been taken to reduce noise to signal ratio and extract the background influence (note that at this energy the DCS decreases for about three orders of magnitude from 10° to 100°).

Although the SCAR procedure improves the IAM method it still suffers from an overestimation of DCSs at small angles, which was the reason for introducing the SCARN procedure to account for this effect (see section 3). It is, off course, important to compare both these methods (SCAR and SCARN) against experiment. However, measurements of DCSs at very small angles (below 20°) are challenging considering the strong influence of the high-current incident electron beam, background scattering and a variation of the effective scattering volume, which overall can result in less accurate results. Therefore, in the present work we have obtained experimental results in the low angular range at low driving pressures and only at higher incident electron energies of 200 eV and 300 eV, where the electron beam is better

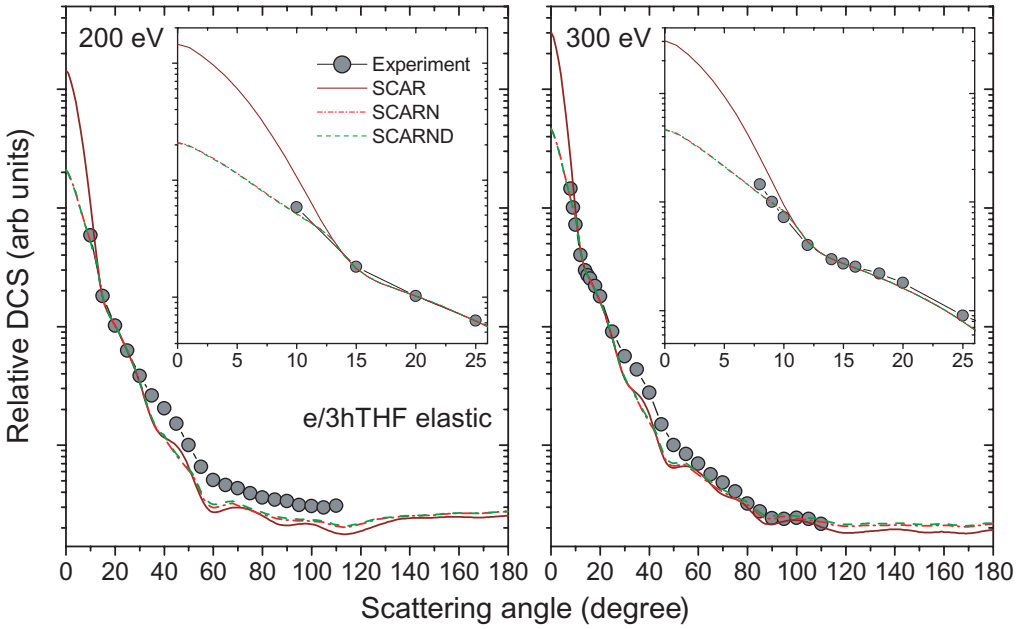

Figure 3. Comparison of relative experimental DCSs for elastic electron scattering from 3hTHF (full circles) with the theoretical results obtained by SCAR (full line), SCARN (dash–dotted line) and SCARND (dashed line) procedures. The relative cross sections are normalized at the scattering angles of 20° for 200 eV and 15° for 300 eV. Insets show the enlarged low-angular region. The errors of the experimental relative cross sections are within the size of the symbols.

focused thus reducing abovementioned influences. The scattering volume corrections were checked against benchmark DCSs for Kr, taken under the same experimental conditions and compared with the existing published data by Danjo [17] (according to our knowledge the only existing data in this energy range down to 10°). The comparison of the relative SCAR (full curve) and SCARN (dash-dotted curve) DCSs with the experiment (full circles) is presented in figure 3. The theoretical curves are here strictly normalized at the angles of 20° (for 200 eV) and 15° (for 300 eV) to obtain accurate comparison in the low-angular region. This leads to a very good agreement in the angular range from about 15° to 30° but a small underestimation of the theoretical DCSs above 40° for 200 eV and in the range from 30° to 50° for 300 eV (note the logarithmic scale). Also, for both energies the calculations show more pronounced shoulders at higher angles. In the low-angular range, as explained above, the theoretical curves diverge significantly (see the insets in figure 3). According to the present measurement, the SCAR procedure clearly overestimates the real DCS values, already starting from about 10°. The corrected SCARN curves are closer to experimental points. Still, the measurements (especially at 300 eV taken in small steps down to 8°) suggest that the SCARN procedure could result in a slight deviation from the real DCS shape and finally in an underestimation of the real values at very small angles. Therefore, although SCARN is in better accordance with the ICSs, for a definite conclusion about a procedure to correct the IAM method at low scattering angles further measurements are needed, which should be performed both in the forward and backscattering directions by applying other experimental methods.

Finally, the relative DCSs for 200 eV and 300 eV obtained by the SCARND procedure are also presented in figure 3 (dashed curves). Note that SCARND DCSs have been obtained by applying the dipole correction (see section 3) to SCARN data, to which they should be compared. It is clear that SCARND results overlap the SCARN ones in the whole angular region, thus showing that at high energies the SCARND procedure does not lead to a deviation of the shape of the cross sections.

4.2. Absolute DCSs

The absolute DCSs for elastic scattering of electrons from the 3hTHF molecule have been experimentally obtained according to relative flow measurements using Kr as a reference gas (see section 2) and are tabulated for the incident electron energies of 40, 50, 100, 150, 200, 250 and 300 eV, in the overall angular range from 8° to 110°. The absolute DCSs have been measured by the relative flow procedure at the energies of 40, 100, 150 and 200 eV, at several scattering angles, while absolute DCSs at the other three tabulated energies (50, 250 and 300 eV) have been obtained according to the normalized relative DCSs independently measured as a function of the incident energy at the fixed scattering angles of 50° and 110° (see the next subsection for details). Apart from experimental challenges connected with the relative flow method (see section 2), the accuracy of the final absolute values also depends on the used reference cross section dataset. Among the existing papers reporting the absolute DCSs for elastic electron–Kr scattering in the energy range of interest for the present work, we have decided to use for the reference data set only those where absolute cross sections have been independently measured, as follows: Williams and Crowe [19] (phaseshift analysis), Srivastava *et al* [18], Danjo [17] and Cho *et al* [25] (relative flow measurements). The final used reference DCSs were then derived as an arithmetic mean of the published values. This should statistically give a more accurate data set derived from several independent measurements. This is especially important considering that the published absolute results by different authors are not always in a perfect agreement, the difference between the lowest and the highest value being even 50% of the mean value at some incident energies and scattering angles. The results of Srivastava *et al* [18] and Cho *et al* [25] are published at energies up to 100 eV, those of Danjo [17] up to 200 eV and by Williams and Crowe [19] up to 400 eV. Finally, the obtained absolute DCSs for 3hTHF by the relative flow method should be consistent with independently measured relative energy and angular distributions, which is an additional check for possible errors in both relative measurements and reference DCSs for Kr.

The present experimental absolute elastic DCSs for 3hTHF are tabulated in table 1 and presented in figure 4 (full circles). The absolute experimental DCS values obtained directly by the relative flow measurements, which were used for calibration, are also shown (open stars). The latter fits very well to the shape of the DCSs measured as a function of the angle. The present experimental absolute DCSs for 3hTHF at all energies either overlap or are slightly below the DCSs for the THF molecule [10] (open squares). The only small change of the absolute DCSs upon substitution of the H atom in THF by the OH group is also confirmed by IAM calculations (not presented here for THF). Still, it would be expected that the DCSs for 3hTHF are somewhat higher on the absolute scale, considering the sizes of the molecules. Although the uncertainty of the absolute measurements does not allow a fine comparison of the absolute DCSs, it seems that the present results for 3hTHF are generally either equal to or slightly below those for THF [10]. It is very interesting that the most recent measurements in the low-energy region [9]

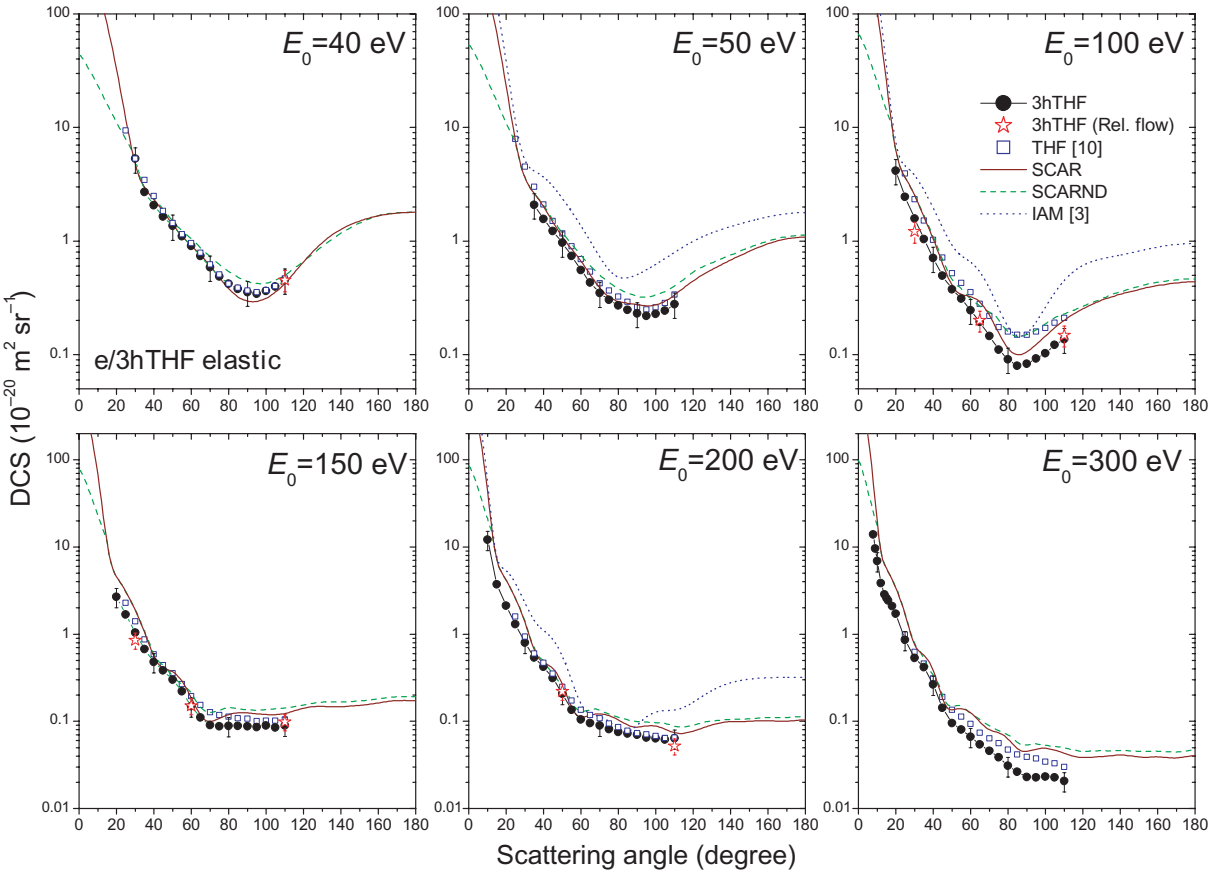

Figure 4. Angular dependence of absolute DCSs for elastic electron scattering from the 3hTHF molecule at different incident energies. The final experimental results (full circles) are presented together with the values obtained directly by relative-flow measurements (open stars). The present calculated absolute cross sections are obtained by SCAR (full line) and SCARND (dashed line) procedures. Dotted lines represent the existing theoretical results for 3hTHF by Možejko and Sanche [3]. The experimental absolute cross sections for the THF molecule by Milosavljević *et al* [10] are represented by open squares.

also showed lower absolute values in comparison with existing THF data, although there this difference is more significant than in the present case (except at the highest used energy of 20 eV). The authors of [9] suggested that a possible reason for this could be a hot target beam (about 90°), inducing most of the target molecules to be vibrationally excited, as well as the presence of several different conformers in the beam. Off course, this possibility cannot be excluded in the present measurements either. It should be noted, however, that we have applied about 20 °C lower heating temperatures, so the effect should be less important. Furthermore, a small influence of impurities in the sample and in the gas lines is also possible (due to the very low vapor pressure of 3hTHF it is more difficult to obtain a pure target beam than in the case of THF). However, this cannot be seen in the shape of the DCSs. A possible systematic shift of the reference DCS data set for Kr also cannot be excluded but should be avoided by using several independent reference results. Finally, one cannot exclude the possibility that existing absolute

Table 1. Experimentally obtained DCSs for elastic electron scattering from 3hTHF in units of 10^{-20} m^2 sr^{-1} as a function of scattering angle (θ) and incident energy (E_0). The absolute errors of relative cross sections (statistical, short-term stability and uncertainty of the effective scattering volume) in the last significant digits are given in parentheses. The errors of the absolute cross sections are estimated to be up to 25% (see section 2 for detailed error discussion).

	E_0(eV)						
θ(°)	40	50	100	150	200	250	300
8	–	–	–	–	–	–	13.9(1.4)
9	–	–	–	–	–	–	9.58(96)
10	–	–	–	–	12.1(1.2)	–	6.89(69)
12	–	–	–	–	–	–	3.82(27)
14	–	–	–	–	–	–	2.84(20)
15	–	–	–	–	3.73(30)	–	2.58(18)
16	–	–	–	–	–	–	2.42(17)
18	–	–	–	–	–	–	2.09(15)
20	–	–	4.17(17)	2.665(80)	2.110(84)	1.711(60)	1.716(86)
25	–	–	2.449(98)	1.668(50)	1.295(52)	0.975(34)	0.859(43)
30	5.30(21)	–	1.573(63)	1.037(31)	0.795(32)	0.608(21)	0.533(27)
35	2.69(11)	2.083(83)	1.039(42)	0.673(20)	0.540(22)	0.445(16)	0.415(21)
40	2.063(83)	1.556(62)	0.706(28)	0.480(14)	0.423(17)	0.323(11)	0.263(13)
45	1.641(66)	1.221(49)	0.496(20)	0.384(12)	0.313(13)	0.2039(71)	0.1422(71)
50	1.355(54)	0.962(38)	0.375(15)	0.3012(90)	0.2068(83)	0.1285(45)	0.0953(48)
55	1.099(44)	0.738(30)	0.311(12)	0.2191(66)	0.1353(54)	0.0991(35)	0.0800(40)
60	0.902(36)	0.556(22)	0.2451(98)	0.1490(45)	0.1047(42)	0.0903(32)	0.0665(33)
65	0.736(29)	0.430(17)	0.1936(77)	0.1108(33)	0.0952(38)	0.0798(28)	0.0540(27)
70	0.589(24)	0.347(14)	0.1461(58)	0.0903(27)	0.0893(36)	0.0673(24)	0.0459(23)
75	0.485(19)	0.302(12)	0.1103(44)	0.0870(26)	0.0810(32)	0.0596(21)	0.0387(19)
80	0.421(17)	0.270(11)	0.0908(36)	0.0881(26)	0.0750(30)	0.0524(18)	0.0307(15)
85	0.377(15)	0.2466(99)	0.0795(32)	0.0880(26)	0.0719(29)	0.0468(16)	0.0263(13)
90	0.354(14)	0.2299(92)	0.0826(33)	0.0875(26)	0.0698(28)	0.0413(14)	0.0230(12)
95	0.344(14)	0.2196(88)	0.0919(37)	0.0858(26)	0.0648(26)	0.0381(13)	0.0228(11)
100	0.363(15)	0.2276(91)	0.1027(41)	0.0888(27)	0.0634(25)	0.0381(13)	0.0232(12)
105	0.396(16)	0.2437(97)	0.1213(49)	0.0850(26)	0.0616(25)	0.0383(13)	0.0227(11)
110	0.453(18)	0.278(11)	0.1364(55)	0.0893(27)	0.0637(25)	0.0392(14)	0.0206(10)

DCSs for THF are slightly higher on the absolute scale, especially in the regions of very low DCS values due to possible higher influence of the background, as explained in the previous subsection. Nevertheless, it is important to point out that possible variations of DCSs should be below the absolute uncertainty.

The experimental results for 3hTHF are compared in figure 4 with the previously published calculations obtained by IAM [3] (dotted curve), as well as with the present SCAR (full curve) and SCARND (dashed curve) calculated DCSs, the latter (SCARND) including both the corrections for the overestimation of DCS at small angles (SCARN) and the rotational excitations. The previous theoretical results [3] are higher on the absolute scale in comparison

with the present data. However, the present calculations and experimental results agree very well. The SCAR calculations are close to experimental DCSs at practically all incident energies within the absolute errors. Interestingly, the SCARND calculations show that the contribution of rotational excitations at 300 K for the 3hTHF molecule is still not absolutely negligible, as the SCARND DCSs are slightly higher (up to about 10%) at all presented energies. However, this puts SCARND DCSs also slightly above experimental DCSs. The SCARND and SCAR, of course, drastically diverge at small angles below about 10°, which is discussed in detail in the previous subsection. Finally, it is interesting to note that even at the lowest used energy of 40 eV, the SCAR DCS practically overlaps the experimental points, showing a wide range of applicability of this approximative method for this type of molecular compounds.

4.3. Energy dependence of the cross sections

The dependence of the absolute DCSs for elastic electron–3hTHF scattering on the incident electron energy, at fixed scattering angles of 50° and 110°, is shown in figure 5. The direct relative measurements performed as a function of the energy are presented by full circles. These relative energy dependent DCSs are normalized to the absolute scale according to the DCS values (open diamonds) extracted from the absolute angle-DCSs, which were calibrated according to relative flow measurements. For both presented scattering angles (50° and 110°), the directly measured energy-dependent DCS curves fit the values extracted from the absolute angle-DCSs very well. The absolute energy dependent DCS at 50° (full circles) has been used to normalize angle-differential DCSs at 50, 250 and 300 eV. Note that after these DCSs were normalized to the absolute scale, the extracted values at 110° agree very well with the measured energy dependence. The recently published experimental results by Vizcaino *et al* at lower energies up to 20 eV are also presented in figure 5 (full squares), as tabulated in [9]. These results generally fit well with the present experimental data.

The calculated DCSs obtained by SCAR (full line) and SCARND (dashed line) procedures are presented in the energy range from 5 eV to 500 eV to compare against experimental results. The theoretical results agree very well with the present measurements, being only slightly higher on the absolute scale, as also shown for angle-DCSs. As expected, the SCARND procedure, which accounts for the rotational excitations, gives somewhat higher absolute DCSs but the difference in comparison with the SCAR calculations is not significant. At the scattering angle of 110° this difference slowly increases with decreasing incident energy. At the scattering angle of 50° the difference is practically negligible down to about 10 eV, where the SCARND DCS significantly decreases which is the consequence of the SCARN method (also included in the SCARND) where corrections are applied to reduce DCSs at small scattering angles. The calculated absolute DCSs at 50° agree very well with the experiment down to about 20 eV but significantly overestimate experimental points of Vizcaino *et al* [9] in the low-energy region. Although it is not expected that the IAM based calculations will be very reliable at low electron energies, it should be noted that the recent theoretical results obtained by the Schwinger multichannel method also overestimate the existing experimental DCSs at low energies in the forward direction, this difference also increases with decreasing energy [9]. However, at the scattering angle of 110°, the present SCAR results agree perfectly with the experiment in the low-energy region. For both given scattering angles in figure 5, the shape of the theoretical DCSs compares very well with the experimentally obtained behavior (except below 20 eV at 50°). It is interesting to note that a small plateau in the DCS curve, revealed by the present

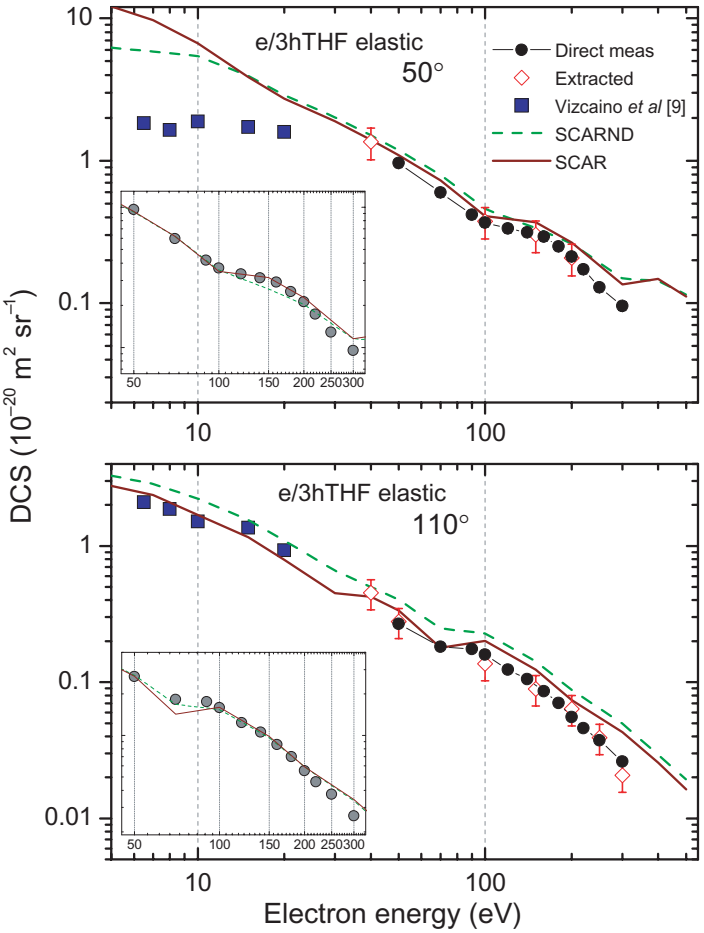

Figure 5. Energy dependence of absolute DCSs for elastic electron scattering from a 3hTHF molecule at the scattering angles of 50° and 110°. Open diamonds: values extracted from the present absolute angle-DCSs; full circles: direct relative measurements as a function of the incident energy, normalized according to extracted absolute values; full squares: existing experimental results by Vizcaino *et al* [9]; full line: SCAR calculations; dashed line: SCARND calculations. Where not shown the errors of experimental values are within the size of the symbols.

experimental points between 100–150 eV at 50° and 80–100 eV at 110°, is also very well reproduced by the calculations (see the insets in figure 5).

In figure 6, the energy dependence of the integral and TCSs for electron collision with 3hTHF is presented. The calculated cross sections are also tabulated in a wide energy range from 5 eV to 10 000 eV in table 2. They include ICS for inelastic electronic processes (dashed curve), ICS for inelastic electronic and rotational processes (dotted curve), elastic ICS (full curve), TCS obtained by the SCAR method (dash–dotted curve) and, finally, TCS obtained by the SCARND procedure which also includes rotational excitations (short-dashed curve). As can be seen in the figure, the estimated influence of the rotational losses, by assuming a model of a free electric dipole (see sections 3), starts to be important below approximately 100 eV and increases with

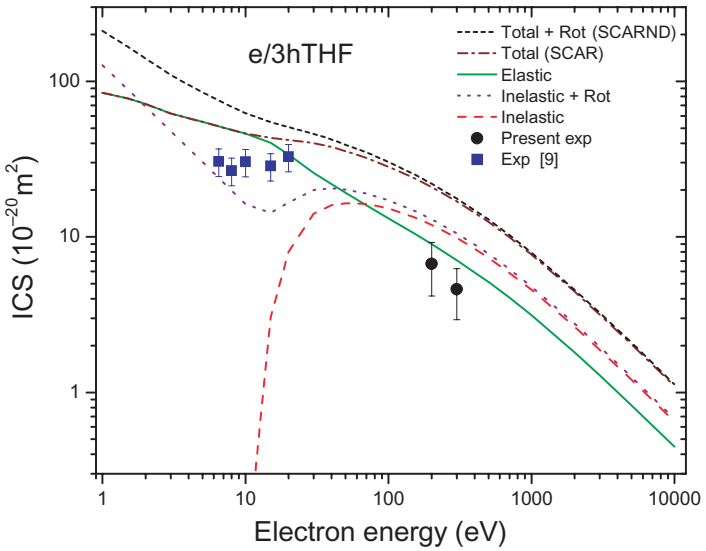

Figure 6. Calculated integral elastic cross section (full line), integral electronically inelastic cross section (dashed line), integral inelastic cross section including rotational excitations (dotted line), TCS (dash–dotted line) and TCS including rotational excitations (short-dashed line) for electron scattering from the 3hTHFA molecule. The present experimental integral elastic cross sections at 200 eV and 300 eV (full circles) and previous ones at lower energies by Vizcaino *et al* [9] (full squares) are presented, as well.

decreasing incident electron energy, resulting in an increase of the TCS by about factor of 2 in the low-energy range. The previous experimental elastic ICSs [9], as tabulated in the paper, are presented by full squares. These ICSs are below the present calculations in the low-energy region (by about a factor of 2) as a consequence of the lower DCS values in the forward direction, which has been discussed in the previous subsection. At the highest reported energy of 20 eV, the ICS reported in [9] agrees perfectly with the present results. It has been already suggested in the paper on THF molecule [14] that DCSs below 50°, due to a steep increase with decreasing scattering angle, introduce about 55% contribution to the ICS. Therefore, ICSs derived after an extrapolation of experimental DCSs which were not measured down to very small angles crucially depend on the shape of the theoretical curve used for the extrapolation. In the present case, there are two possible models available to extrapolate experimental DCS: SCARN and SCAR, which were discussed in the section 4.1 (see figure 3) and can be applied to define minimal and maximal values of the ICS, respectively. However, for the experimental DCS which were measured down to 20° and 30° the variations are very large (above 50%), so the ICSs would not be instructive. For the incident energies of 200 eV and 300 eV, where measurements were performed down to 10°, the uncertainty of the mean ICS value derived according to SCAR and SCARN extrapolation is up to 28%, which is reasonable. These present experimental elastic ICSs are presented in figure 6 by full circles. They are somewhat below the calculated curve, similarly to absolute DCSs which were discussed in the previous subsection. Still, considering the uncertainty of the absolute measurements and the ICS derivation, the overall agreement between the theory and experiment is fairly good.

Table 2. Theoretical integral elastic, integral inelastic and TCSs for electron scattering from 3hTHF in units of $10^{-20}\,m^2$ as a function of incident electron energy (E_0), calculated by using the SCAR method. Integral inelastic and TCSs are also presented with included rotational excitations for a free electric dipole approximation.

E_0 (eV)	Elastic	Inelastic	Inelastic + Rot.	Total	Total + Rot.
5	54.88	0.000	30.24	54.88	85.12
7	50.40	0.000	22.34	50.40	72.80
10	46.20	0.07112	16.24	46.20	62.44
15	40.32	3.052	14.25	43.40	54.60
20	33.88	8.036	16.66	42.00	50.68
30	25.82	14.11	20.05	40.04	45.92
40	21.81	15.96	20.52	37.80	42.28
50	19.26	16.44	20.16	35.56	39.20
70	15.99	16.27	19.01	32.20	35.00
100	13.16	15.23	17.19	28.28	30.24
150	10.56	13.41	14.76	23.97	25.31
200	8.988[a]	11.96	12.99	20.92	21.95
300	7.084[a]	9.828	10.53	16.91	17.61
400	5.908	8.372	8.904	14.28	14.81
500	5.124	7.336	7.784	12.46	12.91
700	4.060	5.852	6.188	9.940	10.28
1000	3.136	4.564	4.788	7.700	7.924
2000	1.812	2.646	2.766	4.452	4.564
3000	1.288	1.882	1.966	3.164	3.248
5000	0.826	1.210	1.260	2.038	2.089
10000	0.448	0.6496	0.6776	1.098	1.126

[a] Experimentally obtained ICSs at 200 eV and 300 eV are 6.7 ± 1.9 and 4.6 ± 1.2, respectively (given uncertainties are only due to different extrapolation of experimental points).

5. Conclusion

The absolute cross sections, both experimental and theoretical, for elastic scattering of electrons from the 3hTHF molecule have been reported. The experimental absolute DCSs were obtained at incident energies from 40 eV to 300 eV, in the overall angular region from 10° to 110°, according to measurement of relative DCSs (as a function of both the scattering angle and the incident energy) and relative flow measurements with Kr as a reference gas. Additionally, elastic ICSs at 200 eV and 300 eV were derived after an extrapolation of the experimental points by using two different present theoretical models. The calculations were performed using the SCAR procedure, with additional data sets where corrections were applied to account for the overestimation of DCS at small angles (SCARN) and to estimate rotational excitations (SCARND). The calculated results include absolute DCSs, ICSs and TCSs in the overall energy range from 5 eV to 10 000 eV.

The present results are discussed regarding the relative shape of the angle-differential DCSs, absolute angle-differential DCSs, absolute energy-differential DCSs and ICSs. Also,

present cross sections are compared with the existing theoretical results [3] and very recent experimental results for 3hTHF [9] reported in the low-energy region up to 20 eV, as well as with the existing recent results for other molecules of similar structure THF [10] and THFA [11]. The calculated DCSs using the SCAR procedure generally agree very well with the experiment, regarding both the shape and the absolute values. Going into detail, the calculated DCSs appear to be slightly above the experimental values on the absolute scale. This was usually still within the experimental errors for the SCAR method but somewhat above for the SCARND procedure which accounts for the rotational excitation, as well. Also, the SCAR method seems to overestimate the DCSs in the low-angular region below about 10°. The newly applied SCARN procedure, which should correct for this effect, although bringing the DCSs closer to the experimental values, seems also to introduce a small deviation to the DCS shape, therefore should be further investigated. Finally, it should be pointed out that the present theoretical method established itself as a powerful tool to calculate elastic electron scattering from the 3hTHF molecule (and other molecules of similar structure), giving a good agreement with experiment, considering both the DCS and ICS shape and the absolute values, in a wide incident energy range, even down to very low energies.

The present experimental absolute DCSs appeared to be either equal to or slightly below the existing experimental results for the THF molecule [10] but the differences were within the absolute experimental errors. It is interesting to note that the most recent results [9] for 3hTHF in the low-energy range also showed lower absolute DCS values in comparison with THF, although much more pronounced than in the present work at the lowest energies and in the forward direction. A definite explanation for this small deviation from the expected calculated behavior (which predicts higher absolute DCSs for 3hTHF) still cannot be given and further possibilities have been also discussed in the present paper. Still, the experiments confirm that the absolute DCSs for THF and 3hTHF are very close on the absolute scale, as was expected. Furthermore, in this work we have also compared the relative shape of the DCS for all three molecules that have been used in recent years to model deoxyribose sugar—THF, 3hTHF and THFA. The DCSs show practically the same behavior at all incident energies. Therefore, in contrast to chemical characteristics and excitation processes, a substitution of the H atom attached to the furanose ring in THF by a group of atoms (OH or C_2OH) practically negligibly affects the elastic scattering process in the present incident energy range.

The present results contribute to a fundamental understanding of elementary processes of electron interaction with various molecular species of furanose structure. They are also important for testing possible theoretical procedures to calculate reliable cross sections for electron–molecule interactions in the medium incident electron energy range. Furthermore, the tabulated absolute cross sections for the 3hTHF molecule, which is structurally similar to building blocks of DNA (RNA), can be used as starting parameters for energy deposition modeling in biologically relevant media and radiation damage research.

Acknowledgments

We are very grateful to Dr Pawel Możejko from Gdansk University of Technology for sending us calculated results in numerical form. Also, we are deeply grateful to Professor Mariusz Zubek from Gdansk University of Technology for the references on gas-kinetic diameters and a very useful and fruitful discussion on relative flow measurements. This work has been partially supported by the Ministry of Science and Technological Development of Republic

of Serbia under project 141011 and the Spanish Ministerio de Educacion y Ciencia (project BFM2003-04648/FISI) and motivated by research within COST Actions P9 'Radiation Damage in Biomolecular Systems' and CM0601 'Electron Controlled Chemical Lithography (ECCL)'.

References

[1] Michael D and O'Neil P 2000 *Science* **287** 1603
[2] Boudaiffa B, Cloutier P, Hunting D, Huels M A and Sanche L 2000 *Science* **287** 1658
[3] Možejko P and Sanche L 2005 *Radiat. Phys. Chem.* **73** 77
[4] Antic D, Parenteau L, Lepage M and Sanche L 1999 *J. Phys. Chem.* B **103** 6611
[5] Antic D, Parenteau L and Sanche L 2000 *J. Phys. Chem.* B **104** 4711
[6] Ibãnescu B C, May O, Monney A and Allan M 2007 *Phys. Chem. Chem. Phys.* **9** 3163
[7] Zecca A, Chiari L, Sarkar A and Brunger M J 2008 *J. Phys. B: At. Mol. Opt. Phys.* **41** 085201
[8] Papp P, Mach P, Urban J and Matejčík Š 2008 *Facta Universitatis Ser. Phys. Chem. Technol.* **6** at press
[9] Vizcaino V, Roberts J, Sullivan J P, Brunger M J, Buckman S J, Winstead C and McKoy V 2008 *New J. Phys.* **10** 053002
[10] Milosavljević A R, Giuliani A, Ševic D, Hubin-Franskin M-J and Marinković B P 2005 *Eur. Phys. J.* D **35** 411
[11] Milosavljević A R, Blanco F, Ševic D, Garcia G and Marinković B P 2006 *Eur. Phys. J.* D **40** 107
[12] Milosavljević A R, Madžunkov S, Šević D, Čadež I and Marinković B P 2006 *J. Phys. B: At. Mol. Opt. Phys.* **39** 609
[13] Allan M 2007 *J. Phys. B: At. Mol. Opt. Phys.* **40** 3531
[14] Dampc M, Milosavljević A R, Linert I, Marinković B P and Zubek M 2007 *Phys. Rev.* A **75** 042710
[15] Milosavljević A R, Kelemen V I, Filipović D M, Kazakov S M, Pejčev V, Šević D and Marinković B P 2005 *J. Phys. B: At. Mol. Opt. Phys.* **38** 2195
[16] Cvejanović D and Crowe D A 1997 *J. Phys. B: At. Mol. Opt. Phys.* **30** 2873
[17] Danjo A 1988 *J. Phys. B: At. Mol. Opt. Phys.* **21** 3759
[18] Srivastava S K, Tanaka H, Chutjian A and Trajmar S 1981 *Phys. Rev.* A **23** 2156
[19] Williams J F and Crowe A 1975 *J. Phys. B: At. Mol. Phys.* **8** 2233
[20] Nickel J C, Mott C, Kanik I and McCollum D C 1988 *J. Phys. B: At. Mol. Opt. Phys.* **21** 1867
[21] Nickel J C, Zetner P V, Shen G and Trajmar S 1989 *J. Phys. E: Sci. Instrum.* **22** 730
[22] Brnstein Zahlenwerte und Funktionen. Bd I. 1950 *Atom und Molekularphysik 1. Atome und Ionen* (Berlin: Springer)
[23] Blanco F and García G 2003 *Phys. Lett.* A **317** 458
[24] Muñoz A, Oller J C, Blanco F, Gorfinkiel J D, Limão-Vieira P and García G 2007 *Phys. Rev.* A **76** 052707
[25] Cho H, McEachran R P, Tanaka H and Buckman S J 2004 *J. Phys. B: At. Mol. Opt. Phys.* **37** 4639–45